

Roughness and Giant Magnetoresistance in Fe/Cr Superlattices

Eric E. Fullerton, David M. Kelly, J. Guimpel,^(a) and Ivan K. Schuller

Physics Department, 0319, University of California, San Diego, La Jolla, California 92093-0319

Y. Bruynseraede

Laboratorium voor Vaste Stof Fysika en Magnetisme, Katholieke Universiteit Leuven, B-3001 Leuven, Belgium

(Received 11 April 1991)

We have performed detailed studies of the structure, magnetotransport, and magnetization of Fe/Cr superlattices as a function of systematic changes in interfacial roughness. The results clearly show that the giant magnetoresistance is enhanced by the presence of roughness. This fact indicates that interfacial roughness should be explicitly included in theoretical calculations and experimental characterization of superlattices exhibiting giant magnetoresistance.

PACS numbers: 73.50.Jt, 75.50.Rr, 75.70.Cn, 75.70.Fr

The discovery of giant magnetoresistance (MR) in Fe/Cr superlattices has produced much interesting experimental and theoretical work [1–11]. In the original work, MR as high as 50% was reported and shown to be correlated with antiferromagnetic coupling between the Fe layers [1]. Further studies have reported that the saturation field H_S , the magnitude of the normalized magnetoresistance $\Delta R/R$, defined as the change of resistance with applied field divided by the resistance of the sample at saturation, and the antiferromagnetic coupling exhibit oscillatory behavior as a function of Cr thickness t_{Cr} , for fixed Fe thickness t_{Fe} [4]. A number of theoretical approaches have proposed that the Fe-layer antiferromagnetic coupling arises from exchange coupling and that the giant MR is due to spin-dependent scattering [3,6–11]. We show here detailed structural and magnetic data which prove conclusively that in sputtered Fe/Cr superlattices the giant MR *increases* substantially with *increasing* interfacial roughness. The presence of roughness is crucial and should be an essential ingredient in theories explaining the giant MR effect.

In this work, more than one hundred Fe/Cr superlattices were studied as a function of the most important growth parameters controlling the structure and interface of the layers. The superlattices were prepared using dc magnetron sputtering (base pressure of $< 5 \times 10^{-7}$ Torr) on ambient temperature Si and sapphire substrates attached to a computer-controlled rotating platform [12]. Care was taken in assuring that the particle beams were properly shielded to avoid cross talk, the rates remained constant during sample preparation, and the particle beams were not shuttered during sample growth to avoid possible rate oscillations due to plasma instability. Ion-mill Auger-electron spectroscopy on similar samples prepared in the same sputtering system, over the last twelve years, shows that beyond ≈ 100 Å from the surface, oxygen and carbon contamination are below detectable limits [13]. The interface roughness was varied by three independent methods; changing sputtering gas pressure, varying sputtering power, and increasing the total thickness of the superlattice. In all three cases, the structure depends sensitively on the growth conditions. The

samples' structure was thoroughly characterized by high- and low-angle x-ray diffraction. The magnetotransport was measured at liquid helium and room temperatures in fields up to 50 kG on samples of well defined geometry which were photolithographically patterned to allow four-lead resistivity measurements. The magnetization was obtained from SQUID and vibrating-sample magnetometry at helium and room temperature, respectively.

Figure 1(a) shows standard low-angle θ - 2θ x-ray-

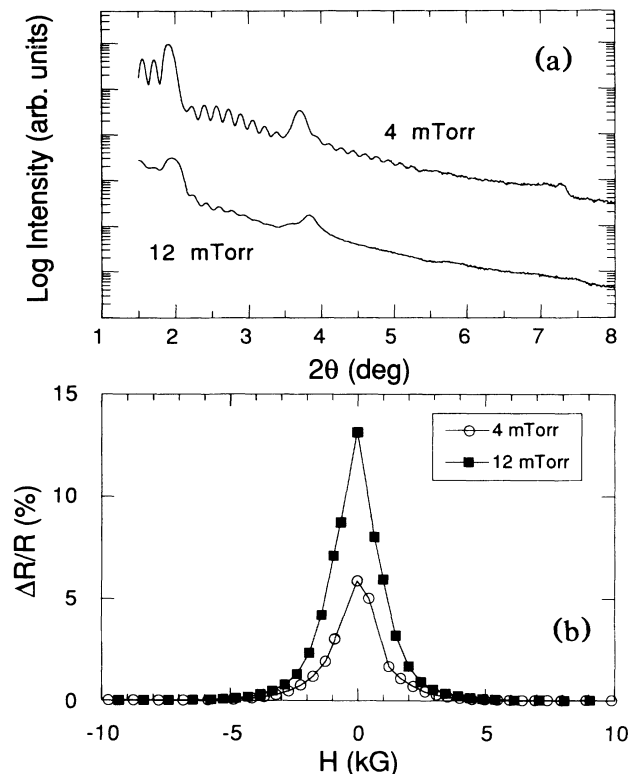


FIG. 1. (a) Low-angle θ - 2θ x-ray-diffraction spectra and (b) $\Delta R/R$ vs applied field at 4 K for selected representative $[\text{Fe}(30 \text{ \AA})/\text{Cr}(18 \text{ \AA})]_{10}$ superlattices sputtered at various Ar pressures. X-ray spectra are offset by two decades for clarity. Saturation resistivities are 26 and 23 $\mu\Omega \text{ cm}$ for the 4- and 12-mTorr samples, respectively.

diffraction spectra of $[\text{Fe}(30 \text{ \AA})/\text{Cr}(18 \text{ \AA})]_{10}$ superlattices, where the subscript is the number of bilayers. The samples were deposited under similar conditions except for the pressure of the Ar sputtering gas, which was changed from 4 to 12 mTorr. The 4-mTorr samples exhibit clear superlattice Bragg peaks up to the second order, a shoulder at the position corresponding to the fourth-order peak, and clean-cut finite-size peaks between the Bragg peaks (the third-order peak is expected to be suppressed because the ratio of Fe to Cr is almost 2:1). The finite-size peaks result from interference of x-ray reflections from the film surface and the film-substrate interface with the periodicity of the peaks determined by the total film thickness. The Bragg and finite-size peaks in the 12-mTorr samples have a considerably reduced intensity and are visibly broadened. The *immediate, qualitative* conclusion is that the 4-mTorr sample exhibits layers which are considerably flatter than the 12-mTorr sample. The broadening of the superlattice Bragg peaks and the loss of higher-order finite-size peaks is characteristic of increased layer roughness [14,15] (i.e., cumulative random variations in layer thicknesses) and not interdiffusion at the interfaces. Low-angle x-ray diffraction typically averages coherently over lateral length scales greater than 1000 \AA [14,15]. The exact nature of the roughness and the characteristic lateral distance is presently under study. The crystal structure determined from high-angle x-ray scan was less sensitive to changes in growth conditions. The films are predominantly bcc (110) oriented with a grain size of 140 and 120 \AA for the 4- and 12-mTorr samples, respectively, obtained from the bcc (110) peak width. The mosaic spreads, determined from the rocking curve full width at half maximum, are 9.5° and 10.5° for the 4- and 12-mTorr samples, respectively.

We should point out that a detailed, *quantitative* interpretation of small-angle x-ray diffraction is not possible at the present time due to the lack of understanding of dynamical corrections [14–17]. A better *quantitative* interpretation of the interfacial disorder would result from the use of high-angle diffraction [14–17] together with nonlinear refinement techniques [14]. Unfortunately, we cannot apply this technique here due to the low contrast in scattering power and similar lattice parameters in Fe/Cr superlattices, which renders the high-angle x-ray data insensitive to interfacial disorder. The conclusions presented here, however, are of a *general, qualitative* nature and do not require sophisticated structural arguments [14].

An inspection of the magnetoresistance ratio $\Delta R/R$ versus magnetic field in Fig. 1(b) shows that the maximum value of $\Delta R/R$ increases substantially with increasing roughness of the layers. Samples sputtered at intermediate Ar pressures show a monotonic degradation of the x-ray spectra and an increase in $\Delta R/R$ with increased Ar pressure. A similar conclusion is obtained as a function of Fe sputtering power. Samples sputtered at higher

Fe target power show visibly narrower and more intense Bragg and finite-size peaks. Reducing the Fe target power from 2.0 kW (0.5 kV, 4.0 A, 10 $\text{\AA}/\text{sec}$) to 0.6 kW (0.4 kV, 1.5 A, 3 $\text{\AA}/\text{sec}$) results in the same qualitative changes in the low-angle x-ray spectra as increasing the Ar pressure shown in Fig. 1(a). $\Delta R/R$ again tracks with the increase of roughness, increasing from 6% to 11% with decreasing Fe target power.

We should stress that all these qualitative structural changes can be understood from standard thin-film growth theory and have been observed in other superlattice systems [18,19]. Because of the sensitivity of the magnetoresistance to growth conditions, the comparison of the results presented in Figs. 1–4 are made on samples for which extreme care was taken to keep all except one of the sputtering parameters constant. The structure of these films should also be sensitive to other sputtering parameters including target-substrate distance, substrate material and temperature, and the presence of initial buffer layers.

The observed dependence of the x-ray spectra and $\Delta R/R$ on the number of bilayers N is somewhat more complicated. Ordinarily in a superlattice without any inhomogeneities, it is expected that the intensity of the low-angle Bragg peaks would increase and then saturate with increasing number of layers. Contrary to expectations, the superlattice Bragg peaks broaden, their intensity decreases, and the nonspecular diffuse scattering increases with increasing N , indicating that the superlattice roughness increases cumulatively with increasing N . It should be pointed out that this implies that the layers close to the substrate are flatter than those further away; consequently the superlattice exhibits changes in roughness across the stack. Again, $\Delta R/R$ is larger for the rougher samples. Some caution should be exercised in interpreting these data since some of the theories developed to date predict an increase in $\Delta R/R$ with increasing N [9]. With this caveat, the fact remains that with increasing roughness the magnetoresistance increases.

A qualitative illustration of the relationship between $\Delta R/R$ and roughness is its dependence on the intensity of the first-order Bragg peak, I_p , which is expected to decrease with increasing roughness. Figure 2 shows that increasing roughness always results in increased magnetoresistance at a variety of Cr thicknesses. For all Cr thicknesses investigated, where antiferromagnetic coupling was maintained, increasing the roughness by increasing the Ar pressure *always* resulted in an enhancement of the $\Delta R/R$. The same trend is observed for samples with a fixed modulation wavelength, using three methods of controlling the roughness: increasing the Ar pressure, decreasing the Fe gun power, and increasing the number of bilayers, N . In all cases, *increasing* roughness always resulted in *enhanced* magnetoresistance.

The magnetization properties, in general, show a weaker dependence on roughness than the magnetoresistance. The saturation moment M_{sat} of the 30- \AA -thick Fe layers

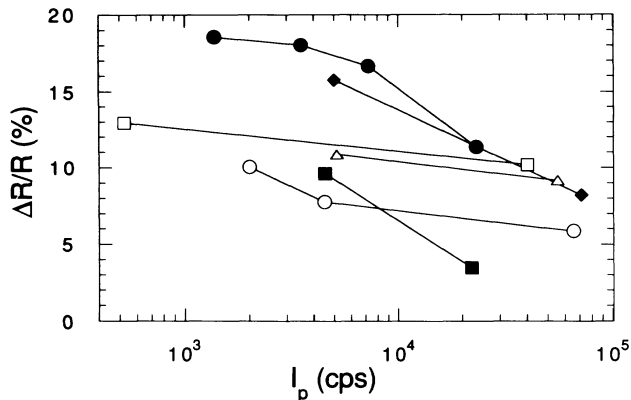


FIG. 2. Dependence of $\Delta R/R$ on the first superlattice Bragg peak intensity I_p for samples with $N=40$. I_p is a qualitative measure of the interfacial roughness (the background intensity has been subtracted). Δ , [Fe(30 Å)/Cr(13 Å)]; \blacklozenge , [Fe(30 Å)/Cr(15 Å)]; \square , [Fe(30 Å)/Cr(16 Å)]; \bullet , [Fe(30 Å)/Cr(18 Å)]; \circ , [Fe(30 Å)/Cr(20 Å)]; \blacksquare , [Fe(30 Å)/Cr(25 Å)].

varied from 1500 to 1700 emu/cm³ and was independent of the roughness or Cr thickness. The small change in M_{sat} implies that the interdiffusion at the interface is not changing significantly with increased roughness. Shown in Fig. 3(a) is the in-plane magnetization curve for the samples presented in Fig. 1. In Fig. 3(b) we show in-plane magnetization curves for samples with the same modulation wavelength as in Fig. 3(a) but different numbers of bilayers. The magnetization curves show the characteristic shearing and low remanent moment resulting from the antiferromagnetic coupling of the Fe layers [3]. The rougher sample in Fig. 3(a) (higher Ar pressure) has increased coercivity and remanent moment with little change in the saturation field. We would like to stress that the increased remanent moment would be expected to decrease the magnetoresistance contrary to what is observed. This shows that the changes in $\Delta R/R$ are not simply resulting from changes in the amount of the sample coupling antiferromagnetically. The increase in the remanent moment most likely occurs from variations in the Cr thickness resulting in regions of the sample that are coupled ferromagnetically. When disorder is introduced only in the Fe layer (by lowering the Fe target voltage), there is no change in the remanent moment. Shown in Fig. 3(b) are the magnetization curves for the $N=5$ and $N=100$ samples. With increased N , there is a small increase in the remanent moment and saturation field without other qualitative changes in the magnetization curves.

Shown in Fig. 4 are the absolute resistivity and magnetoresistance versus t_{Cr} for a series of $N=10$ and $N=40$ superlattices sputtered under similar conditions. For all Cr thicknesses the rougher samples ($N=40$) show a higher magnetoresistance. This behavior is also observed in samples grown at different sputtering pressures and powers for various t_{Cr} , as long as the antiferromagnetic order between the Fe layers is maintained. It is impor-

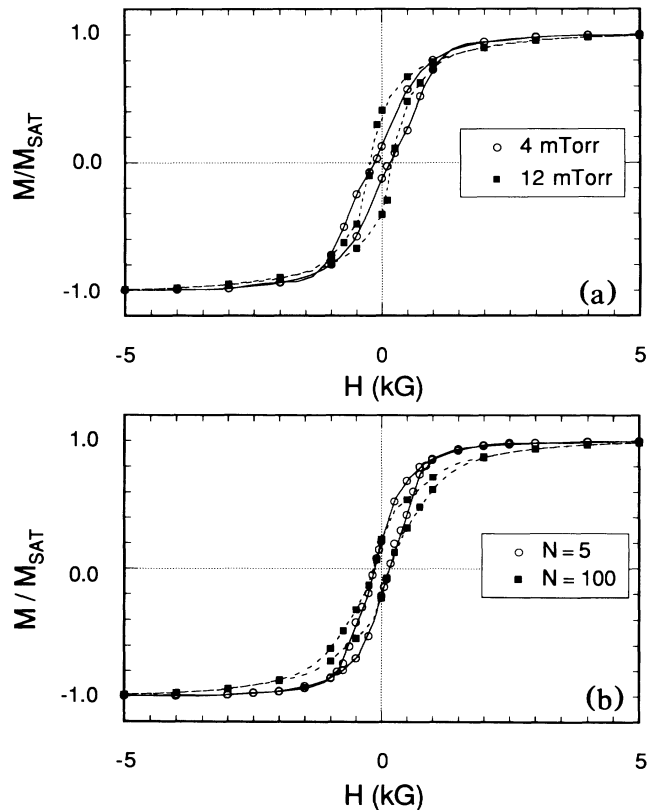


FIG. 3. In-plane magnetization curves normalized to the saturation value (M_{sat}) at 10 K for (a) the same [Fe(30 Å)/Cr(18 Å)]₁₀ samples shown in Fig. 1 and (b) two samples of the same modulation, [Fe(30 Å)/Cr(18 Å)]_N, with $N=5$ and 100. The diamagnetic signal of the substrate has been subtracted from the curves. Lines are guides to the eye.

tant to investigate the absolute changes in resistivity ρ to understand the origin of the changes in $\Delta R/R$. The saturation resistivities of the $N=10$ and 40 samples exhibit a monotonic increase with t_{Cr} at fixed $t_{\text{Fe}}=30$ Å as shown in the inset of Fig. 4. The fact that the dependence of the resistivity on t_{Cr} is systematic and exhibits little scatter also indicates that the growth conditions are stable from sample to sample. The increase in the resistivity with increasing t_{Cr} implies that interface scattering does not dominate the spin-independent scattering in contrast to other superlattice systems [20].

A comparison of these results to the available theoretical calculations is somewhat difficult because most theories fail to explicitly calculate $\Delta R/R$ as a function of roughness. For the samples shown in Figs. 1–4, the saturation resistivities change by less than 15% with increased roughness whereas the spin-dependent scattering (characterized by $\Delta\rho$) increases by as much as 300%, indicating that the spin-dependent scattering is much more sensitive to the interface roughness. This is in qualitative agreement with calculations [8,11] that attribute the giant MR to the spin-dependent random potential at the interfaces. Theoretical results obtained by solving the Boltzmann

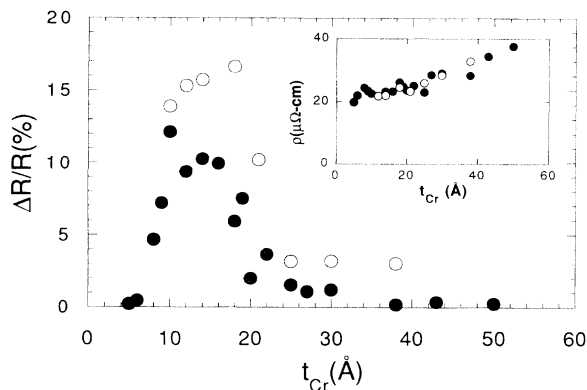


FIG. 4. $\Delta R/R$ vs t_{Cr} for $[\text{Fe}(30 \text{ \AA})/\text{Cr}(t_{Cr})]_N$ superlattices, with $N=10$ (●) and $N=40$ (○). Inset: ρ vs t_{Cr} for the same samples.

transport equation including spin-dependent interfacial scattering [9] predict an increasing magnetoresistance with increasing diffuse interface scattering (i.e., increasing roughness) also in agreement with our experimental results. An increasing magnetoresistance with roughness has also been claimed in a model in which the coupling between the ferromagnetic layers is due to the s electrons in the Cr layer [10]. Clearly further theoretical calculations where the interfacial roughness is explicitly included and comparison with experiments are needed.

In conclusion, we have performed detailed studies of the structure, magnetotransport, and magnetization of sputtered Fe/Cr superlattices as a function of systematic changes in interfacial roughness. The results clearly indicate that the giant magnetoresistance is enhanced by the presence of roughness.

We thank P. Levy, S. Zhang, and N. Garcia for useful conversations and P. Belien for some magnetoresistance measurements. Work supported by U.S. DOE Grant No. DE-FG03-87ER45332 at UCSD and Grant No. 88/93-130 of the Belgian Concerted Action (G.O.A.) and Interuniversity Attraction Poles (IUAP) Programs at KUL. International travel was provided by NATO. Some international travel (J.G.) was provided by a fellowship from CONICET, Argentina.

(a) On leave from Centro Atómico Bariloche, San Carlos de Bariloche, Río Negro, Argentina.

- [1] M. N. Baibich, J. M. Broto, A. Fert, F. Nguyen Van Dau, F. Petroff, P. Etienne, B. Greuzet, A. Friederich, and J. Chazelas, *Phys. Rev. Lett.* **61**, 2472 (1988).
- [2] J. J. Krebs, P. Lubitz, A. Chaiken, and G. A. Prinz, *Phys. Rev. Lett.* **63**, 1645 (1989).
- [3] A. Barthélémy, A. Fert, M. N. Baibich, S. Hadjoudj, F. Petroff, P. Etienne, R. Cabanel, S. Lequien, F. Nguyen Van Dau, and G. Creuzet, *J. Appl. Phys.* **67**, 5908 (1990).
- [4] S. S. P. Parkin, N. More, and K. P. Roche, *Phys. Rev. Lett.* **64**, 2304 (1990).
- [5] S. Araki and T. Shinjo, *Jpn. J. Appl. Phys.* **29**, L621 (1990).
- [6] G. Binasch, P. Grünberg, F. Saurenbach, and W. Zinn, *Phys. Rev. B* **39**, 4828 (1989).
- [7] B. Dieny, V. S. Speriosu, S. S. P. Parkin, B. A. Gurney, D. R. Wilhoit, and D. Mauri, *Phys. Rev. B* **43**, 1297 (1991).
- [8] P. M. Levy, S. Zhang, and A. Fert, *Phys. Rev. Lett.* **65**, 1643 (1990).
- [9] R. E. Camley and J. Barnás, *Phys. Rev. Lett.* **63**, 664 (1989).
- [10] N. García and A. Hernando, *J. Magn. Magn. Mater.* **99**, L12 (1991).
- [11] J. Inoue, A. Oguri, and S. Maekawa, *J. Phys. Soc. Jpn.* **60**, 376 (1991).
- [12] I. K. Schuller, *Phys. Rev. Lett.* **44**, 1597 (1980).
- [13] For an early study of this type, see I. Banerjee, Q. S. Yang, C. M. Falco, and I. K. Schuller, *Solid State Commun.* **41**, 805 (1982).
- [14] E. E. Fullerton, I. K. Schuller, H. Vanderstraeten, and Y. Bruynseraede, *Phys. Rev. B* (to be published).
- [15] For an early discussion of these issues see, D. B. McWhan, in *Fabrication and Applications of Multilayered Structures*, edited by P. Dhez and C. Weisbuch (Plenum, New York, 1988).
- [16] Y. Shiroishi, C. Sellers, J. E. Hilliard, and J. B. Ketterson, *J. Appl. Phys.* **62**, 3694 (1987).
- [17] K. Takanashi, H. Fujimori, H. Watanabe, M. Shoji, and A. Nagai, *Mater. Res. Soc. Symp. Proc.* **10**, 397 (1989).
- [18] H. Nagata and S. Seki, *Jpn. J. Appl. Phys.* **29**, 569 (1990).
- [19] K. Meyer, I. K. Schuller, and C. M. Falco, *J. Appl. Phys.* **52**, 5803 (1981).
- [20] See, for instance, T. R. Werner, I. Banerjee, C. M. Falco, and I. K. Schuller, *Phys. Rev. B* **26**, 2224 (1982).